Załącznik nr 3

Autopresentation of scientific accomplishments (autoreferat)

1 Name

Enrico Maria Sessolo

2 Scientific degrees

- Master's degree in astrophysics, University of Padova, Italy, March 2003

  Thesis: *Spectral signatures of a super-strong magnetic field in neutron stars*
  Advisor: Professor Roberto Turolla

- Master's degree in theoretical physics, University of Kansas, Lawrence, USA, August 2007

  Thesis: *Eikonal contributions to ultra high energy neutrino-nucleon cross sections in low-scale gravity models*
  Advisor: Professor Douglas McKay

- Ph.D. degree in physics, University of Kansas, Lawrence, USA, August 2010

  Thesis: *Beyond the Standard Model with supersymmetry*
  Advisor: Professor Danny Marfatia

3 Employment in academic institutions

- June 2010 - July 2010: Instructor of Physics, University of Kansas, Lawrence, USA
- August 2010 - May 2011: Instructor of Physics, Fort Hays State University, Hays, USA
- June 2011 - December 2015: Postdoctoral fellow, National Centre for Nuclear Research, Warsaw

- January 2016 - Present: Assistant professor (Adiunkt), National Centre for Nuclear Research, Warsaw

4 Prolonged academic stays

- February 2017 - November 2017: Humboldt Fellowship for Experienced Researchers, Technische Universitaet Dortmund, Dortmund, Germany

5 Scientific accomplishment

In the sense of article 16, paragraph 2 of the Act on Academic Degrees and Academic Title, and on Degrees and Title in Arts, 14 March 2003 (Dz. U. No 65, item 595 as amended).

a) Title of scientific achievement - a monographic series of publications

Dark matter signatures in models of new physics

b) The monographic series of publications (authors, title, journal, applicant's contribution)

[H1] Leszek Roszkowski, Enrico Maria Sessolo, Yue-Lin Sming Tsai
Bayesian implications of current LHC supersymmetry and dark matter detection searches for the constrained MSSM,
Phys.Rev. **D86** (2012) 095005 (arXiv:1202.1503)

[H2] Kamila Kowalska, Leszek Roszkowski, Enrico Maria Sessolo,
Two ultimate tests of constrained supersymmetry,
JHEP **1306** (2013) 078 (arXiv:1302.5956)

[H3] Leszek Roszkowski, Enrico Maria Sessolo, Andrew J. Williams,
What next for the CMSSM and the NUHM: Improved prospects for superpartner and dark matter detection,
JHEP **1408** (2014) 067 (arXiv:1405.4289)

[H4] Leszek Roszkowski, Enrico Maria Sessolo, Andrew J. Williams,
Prospects for dark matter searches in the pMSSM,
JHEP **1502** (2015) 014 (arXiv:1411.5214)

[H5] Kamila Kowalska, Enrico Maria Sessolo,
The discreet charm of higgsino dark matter - a pocket review,
Adv. High Energy Phys. **2018** (2018) 6828560 (arXiv:1802.04097)

[H6] Leszek Roszkowski, Enrico Maria Sessolo, Sebastian Trojanowski, Andrew J. Williams,
Reconstructing WIMP properties through an interplay of signal measurements in direct detection, Fermi-LAT, and CTA searches for dark matter,
JCAP **1608** (2016) no.08, 033 (arXiv:1603.06519)

[H7] Arghya Choudhury, Kamila Kowalska, Leszek Roszkowski, Enrico Maria Sessolo, Andrew J. Williams,
Less-simplified models of dark matter for direct detection and the LHC,
JHEP **1604** (2016) 182 (arXiv:1509.05771)

[H8] Kamila Kowalska, Enrico Maria Sessolo,
Expectations for the muon g-2 in simplified models with dark matter,
JHEP **1709** (2017) 112 (arXiv:1707.00753)

c) Description of the scientific goals and results of the series of publications with a discussion of possible applications

5.1 Introduction

One of the most important challenges of contemporary physics is to understand the nature of the dark matter (DM) of the Universe. The long-held paradigm is that DM is cold and most likely composed of weakly interactive massive particles, or WIMPs. WIMPs are particles that emerged as a relic from the primordial thermal bath as the early Universe expanded and cooled down after the Big Bang.

In this report of scientific goals I will provide an account of my contribution to the global effort undertaken by particle physicists in the past few years to constrain WIMP properties, in light of the large amount of data that became available at the Large Hadron Collider (LHC), in direct searches for DM with deep underground Xenon detectors, and in indirect DM searches in astrophysical signals.

In spite of null results from virtually all of the experiments designed to seek for DM particles, I will make the point that we have been able to derive valuable information on the possible nature and properties of the WIMP, which can in turn be used to direct future and more meaningful observational strategies and design new experiments.

Finally I will also argue that, while exploring altogether new alternatives to the WIMP paradigm constitutes in itself a healthy and necessary endeavor, the widespread pessimism about the eventual outcome of traditional searches for WIMPs is not warranted by the data but is rather a result of over-optimistic expectations founded on theoretical prejudice, which failed to materialize when confronted with observations. On the contrary, while nobody can obviously guarantee a WIMP discovery at any point in the near future, I believe that, in light of the experimental information we hold now, the prospects for DM detection in existing or approved experiments remain, as we shall see, fairly rosy.

5.2 Brief review of the evidence for dark matter

Before presenting my scientific contribution, featured in the references enumerated at the beginning of Sec. 5, I will briefly remind the reader of the incontrovertible evidence for DM and of the solid theoretical arguments for WIMPs (details are well described in several reviews, *e.g.* [1, 2].)

The first claim about the existence of DM is usually attributed to Zwicky's original paper on the Coma Cluster [3]. The cluster consists of more than a thousand galaxies. Careful analysis of the movement along their gravitational orbits led to the conclusion that there should be a large amount of non-luminous matter contained in the cluster. Following these early observations, one of the most widely recognized arguments for the existence of DM is based on galaxy rotation curves, *i.e.* the relation between orbital velocity and radial distance of visible stars or gas from the center of a galaxy. For example, the velocities of distant stars in the disc M31 remained roughly constant over a wide range of distances from the center of the galaxy, in contradiction with expectations based on the distribution of visible matter in the galaxy. Similar results were later obtained for various other spiral galaxies [4, 5].

The existence of DM is also supported by data coming from gravitational lensing. Gravitational lensing, or the bending of light in a strong gravitational field, is most easily observed when light passes through a very massive and/or dense object, like a galaxy cluster or the central region of a galaxy. Light rays can bend around the object, or lens, leading to a distortion of the image of the light source. To this class belongs perhaps the most spectacular argument for the existence of DM in clusters, which can be found in the Bullet Cluster. It consists of two clusters of galaxies which have undergone a head-on collision [6]. The hot-gas clouds (observed through their X-ray emission) that contain the majority of the baryonic mass in both clusters have been decelerated in the collision, whereas analysis of the gravitational lensing effect shows that the center of mass for both clusters is clearly separated from the gas clouds, as if the movement of the galaxies and the DM halos in clusters remained almost intact. One can thus infer the presence of a large amount of non-collisional mass in both clusters. Studies of weak gravitational lensing of large scale structures provide further evidence for DM.

Last but not least, a crucial role in determining the DM abundance in the Universe is played by studies of cosmic microwave background (CMB) radiation. The CMB radiation seen today originates from the decoupling and recombination epoch. Small inhomogeneities in the distribution of its temperature correspond to fluctuations of the matter density in the early Universe that subsequently gave rise to the observed large structures.

The power spectrum of temperature anisotropies, when expanded in terms of spherical harmonics, depends on cosmological parameters that can then be obtained by fitting the resulting spectrum, with some underlying assumption of cosmological model, *e.g.*, the ΛCDM model. The current value [7] of the relic abundance was obtained by WMAP and more recently by PLANCK by fitting the six-parameter ΛCDM model and reads:

$$\Omega_b\, h^2 = 0.02226(23), \tag{1}$$
$$\Omega_{\rm DM}\, h^2 = 0.1186(20), \tag{2}$$

where Ω_b is the ratio of the density of baryonic matter to the critical density (the energy density corresponding to a flat Universe), the corresponding quantity for the non-baryonic DM component is $\Omega_{\rm DM}$, and $h = H_0/100\,\text{km}\,\text{Mpc}\,\text{s} = 0.678(9)$ is the reduced Hubble constant, with H_0 denoting the Hubble constant *today*. The remaining dominant contribution, $\Omega_\Lambda \approx 0.692$, accounts for the so-called dark energy (for a recent review see [8]).

One clear conclusion that one can draw from observational evidence is that DM is made up of some particles that should be practically electrically neutral. DM should interact with ordinary matter preferably only weakly (or sub-weakly), where weak can be taken to mean the weak nuclear force or just having a (sub)weak but non negligible coupling to the particles of the Standard Model (SM). DM self-interactions cannot be too strong in order to be compatible with constraints on structure formation and observations of galaxy cluster systems such as the Bullet Cluster, with current limits of order $\sigma/m < 0.7\,\text{cm}^2/\text{g}$ [9]. Moreover, to be in agreement with CMB data, most of the DM should be non-baryonic in nature.

One simple classification of DM particles is based on how relativistic they are around the time when they fall out of thermal equilibrium in the early Universe, *i.e.*, when they decouple from the thermal plasma.

Hot DM in the mass range of up to a few tens of eV, which was still relativistic at the time of decoupling, did not cluster to form clumps as small as galaxies due to the large mean free path and does not reproduce the observed Universe in numerical simulations of large scale structure formation.

In contrast, non-baryonic *cold* DM decoupled from the thermal plasma at freeze-out and its density perturbations started growing linearly at the onset of the epoch of matter dominance. This provided early potential wells (seeds), thus triggering and catalyzing the growth of the density perturbations of baryonic matter after it decoupled from radiation some time later. This is the basic reason why cold DM generally proves successful in reproducing observations in numerical simulations of large structure formation, despite some well-known problems (the "missing satellites" problem, referring to the small number of predicted substructures, and the "too-big-to-fail" problem, referring to local overdensities; for a recent review see, *e.g.*, [10]).

As a possible way of ameliorating some of the apparent problems of cold DM, *warm* DM, in the mass range of a few keV, has been considered. Warm DM was still relativistic at the time of decoupling but fluctuations corresponding to sufficiently large halos would not be damped by its free streaming. Because warm DM reduces the power spectrum on small scales, it reduces the missing satellite problem. However this comes at the price of intruducing new inconsistencies on the rate of star formation as inferred from observations of the Lyman-alpha forest (see, *e.g.*, [11]).

An array of these and related arguments have led to establishing a popular (and sensible) paradigm that the dominant fraction of DM is probably cold and that it should be not only (sub)weakly interacting but also non-relativistic and massive or, in short, made up of WIMPs. Finally, the DM particles should be either absolutely stable, or extremely long lived (for instance, a recent analysis finds a lower bound of 160 Gyr [12]).

For completeness I would like to mention that non-WIMP DM candidates (for a recent review see [13]) have also been vastly explored in the literature. Among them one can distinguish an ultralight axion that emerges from the solution to the strong CP problem. Another interesting scenario is to consider extremely weakly interacting massive particles as DM candidates. Such weak interactions can naturally appear if, for example, they are described by non-renormalizable operators suppressed by some high energy scale, *e.g.* the Planck mass, $M_{\mathrm{P}} \approx 10^{19}\,\mathrm{GeV}$, as it is in the case of gravitino DM, or the Peccei-Quinn scale for the axino DM. I will not discuss these scenarios any further.

5.3 Thermal freeze-out

The most popular and arguably most robust mechanism for generating the DM relic abundance is thermal freeze-out. Simply put, in the very early and hot Universe SM species and DM were in thermal equilibrium, with DM particle production and annihilation balancing each other out. As the Universe expanded and cooled, the DM particles eventually froze out of equilibrium with the thermal plasma, when the DM annihilation rate, Γ_{ann}, became roughly less than the expansion rate of the Universe: $\Gamma_{\mathrm{ann}} \lesssim H \sim T_f^2/\overline{M}_P$, where T_f stands for the freeze-out temperature (the index f indicates that quantities are evaluated at the freeze-out time), H is the Hubble constant, and $\overline{M}_P$ is the reduced Planck mass. After freeze-out the DM yield, $Y_{\mathrm{DM}} = n_{\mathrm{DM}}/s$, where n_{DM} is the number density of DM particles and $s \sim T^3$ is the entropy density, remained mostly constant.

After expressing the annihilation rate in terms of the thermally averaged annihilation cross section times particle velocity, $\langle\sigma_{\rm ann}v\rangle$, so that $\Gamma_{\rm ann}=n_{\rm DM}\langle\sigma_{\rm ann}v\rangle$, one can write [14],

$$\Omega_{\rm DM}h^2\simeq\frac{m_{\rm DM}\,n_{\rm DM}(T_0)}{\rho_c}\,h^2=\frac{T_0^3}{\rho_c}\,\frac{x_f}{\overline{M}_P}\,\frac{1}{\langle\sigma_{\rm ann}\bar{v}\rangle_f}\,h^2, \tag{3}$$

where $T_0\approx 2.35\times10^{-13}$ GeV is the temperature of the Universe at present, $\rho_c\approx 8\times10^{-47}\,h^2\,{\rm GeV}^4$ is the critical energy density, $x=m_{\rm DM}/T$ and $\bar{v}=|\vec{v}_1-\vec{v}_2|$ is the relative velocity of the two annihilating DM particles in the center-of-mass frame.

The value of x_f can be roughly estimated by assuming that around freeze-out the DM number density is equal to the non-relativistic equilibrium number density, $n_{\rm eq}=g(x_f/2\pi)^{3/2}e^{-x_f}$, where g is the number of degrees of freedom for the DM particles. Using $\Omega_{\rm DM}\,h^2\approx 0.12$ one obtains

$$x_f^{3/2}e^{-x_f}\approx\frac{10^{-8}\,{\rm GeV}}{m_{\rm DM}}. \tag{4}$$

This leads to $x_f\approx 30$ for $m_{\rm DM}\approx 100\,{\rm GeV}-10\,{\rm TeV}$. More careful analysis shows that the appropriate value is closer to $x_f\approx 25$ [15].

Finally we put the estimated value of x_f back into Eq. (3) and find

$$\langle\sigma_{\rm ann}\bar{v}\rangle_f\approx 3\times10^{-26}\,{\rm cm}^3/{\rm s}. \tag{5}$$

In a precise treatment, which takes into account the dynamics of freeze-out, the DM yield after freeze-out is found by solving the respective set of Boltzmann equations:

$$\frac{d\rho_R}{dt} = -4H\rho_R+\langle\sigma_{\rm ann}\bar{v}\rangle\,\langle E\rangle\big(n_{\rm DM}^2-n_{\rm eq}^2\big), \tag{6}$$
$$\frac{dn_{\rm DM}}{dt} = -3Hn_{\rm DM}-\langle\sigma_{\rm ann}\bar{v}\rangle\big(n_{\rm DM}^2-n_{\rm eq}^2\big), \tag{7}$$

where ρ_R is the radiation energy density and $\langle E\rangle$ is the average energy of annihilating DM particles. As can be deduced from Eq. (7) – and is even more evidently seen from simplified solution (3) – the larger is $\langle\sigma_{\rm ann}\bar{v}\rangle$ at freeze-out the longer the DM stays in thermal equilibrium and therefore the lower relic abundance $\Omega_{\rm DM}h^2$ one obtains.

5.4 WIMP searches in the dark: the naturalness bias

Thermal freeze-out fails to provide information on the nature of the DM itself, as a cross section of the size of Eq. (5) can result from a discouraging wide range of DM mass values, spin quantum numbers, and DM-SM coupling strengths. Thus, in lack of more information, one has almost always to resort to some theoretical assumptions in order to narrow options down.

Until recently the main principle guiding expectations for the physics beyond the SM has been the *gauge hierarchy* (or, simply, hierarchy) problem. Roughly speaking, this is the fact that when a low-energy effective theory includes light fundamental scalar fields like the Higgs boson in the SM the mass of the scalar becomes subject to strong renormalization by the fields of the high-energy, or ultra-violet (UV), completion. If the UV completion's typical scale is, for example, close to the scale of quantum gravity, $\overline{M}_P$, one has to *fine-tune* the Lagrangian input parameters by approximately 28 orders of magnitude to justify a scalar mass of the order of the electroweak symmetry-breaking (EWSB) scale. Thus, one generically expects the new degrees of freedom to be close to the EWSB scale rather than much heavier.

Arguably the most thoroughly studied scenario for new physics is low-scale supersymmetry (SUSY; see, *e.g.*, [16] for a review). This is based on the idea that there is a symmetry associating to every fermion of the SM a bosonic superpartner and viceversa. SUSY provides an attractive solution to the hierarchy problem thanks to the non-renormalization theorem, which precludes one-particle irreducible loop corrections to the superpotential so that, as a consequence, mass terms do not get renormalized. In other words, SUSY "protects" the Higgs mass of the SM and makes it technically natural.

Because of the hierarchy problem, the particles of the minimal supersymmetric Standard Model (MSSM) have been the subject of extensive research for the good part of the last 4 decades. However, a large number of alternatives to SUSY exist, also designed to solve the hierarchy problem. For example, some models consider the Higgs boson not as a fundamental particle, but rather a condensate of a new strong sector with a characteristic $\sim$ TeV scale, which is used to regulate the divergent integrals and prevent the quantum corrections to the Higgs mass from running away (see, *e.g.*, [17] for a modern review on *compositeness*). Others are based on the idea of a "bulk" of additional spatial dimensions (called *extra*-dimensions), compactified along the usual, infinitely extending, three. The natural cut-off to the Higgs mass corrections is in this case provided by the typical scale of quantum gravity in the bulk, which is of the order of a TeV (*e.g.*, [18] and references therein). Others still involve the existence of additional fundamental scalars (*e.g.* [19]) and/or fermions (*e.g.* [20]).

A remarkable consequence of these models is that, simply on dimensional grounds, if one of the expected TeV-scale new particles were stable enough to be the DM, cross section (5) would lead to a coupling with the SM of the size of the electroweak coupling constant. This fascinating coincidence, which, in light if its singling out specifically weakly interacting massive particles, or WIMPs, is known as the "WIMP miracle," has provided for several decades the guiding principle behind the search for DM, and furnishes an enticing theoretical motivation for WIMPs to these days.

On the other hand, it became clear from the early days of the LHC that expectations for new particles and DM driven exclusively by a strict interpretation of the no fine-tuning argument had to be carefully rethought, as the rapid experimental progress from different and complementary fronts put the most natural regions of almost all mentioned models at odds with observations. In the next two subsections I will thus recall, after briefly reviewing a few basic notions on direct DM detection, one specific example that highlights the tension between *naturalness*, or the absence of fine tuning, and recent data. I will then show in the following sections how the same data that put the naturalness idea under pressure has also provided a direction for future searches and understanding.

5.4.1 A note on direct DM detection

One of the most important strategies to search for WIMP DM is its possible detection through elastic scatterings of DM particles off nuclei. For WIMPs that interact efficiently enough with baryons this process can lead to a clear signature in low-background underground detectors.

An evaluation of a DM event rate in underground experiments necessarily involves factors from particle physics and nuclear physics, as well as from astrophysics. This can be seen from the formula for the differential recoil event rate as a function of the recoil energy E_r

$$\frac{dR}{dE_r}(E_r) = \left(\frac{\sigma_0}{2\mu^2\, m_{\mathrm{DM}}}\right) \times F^2(E_r) \times \left(\rho_{\mathrm{DM}} \int_{v\geq v_{\min}}^{v\leq v_{\mathrm{esc}}} d^3v\, \frac{f(\mathbf{v},t)}{v}\right), \tag{8}$$

where σ_0 is the DM-nucleus scattering cross section in the zero momentum transfer limit, m_{DM} is the DM mass, $\mu \equiv m_{\mathrm{DM}}M/(m_{\mathrm{DM}}+M)$ is the reduced mass of the WIMP-nucleus system for nucleus of mass M, $F(E_r)$ is the nuclear form factor of the target nucleus, ρ_{DM} is the local DM density and v is the relative velocity of the DM particle with respect to the nucleus, while $f(\mathbf{v},t)$ denotes the distribution of the WIMP velocity with cut-off at the galaxy escape velocity v_{esc}. The minimum velocity that can result in an event with recoil energy E_r is given by $v_{\min} = (\delta + ME_r/\mu)/\sqrt{2M\,E_r}$, where $\delta = 0$ for elastic scatterings.

Since WIMPs are characterized by non-relativistic velocities, one typically applies the limit $v \to 0$ when calculating the cross section. In this case the corresponding cross section can be decomposed into two contributions: the *spin-independent* and the *spin-dependent* (marked by SI and SD, respectively, in the following formulas): $\sigma^0 F^2(E_r) = \sigma^{\mathrm{SI}} F^2_{\mathrm{SI}}(E_r) + \sigma^{\mathrm{SD}} F^2_{\mathrm{SD}}(E_r)$, where σ^{SI} and σ^{SD} are given at zero momentum transfer. In the absence of isospin violating interactions between DM and nucleons one obtains $\sigma^{\mathrm{SI}} = \sigma_p^{\mathrm{SI}}(\mu^2/\mu_p^2)\,A^2$, where $\sigma_p^{\mathrm{SI}} = (4\mu_p^2/\pi)\,f_p^2$, with μ_p being the reduced mass of the WIMP-proton system and f_p the scattering amplitude. Note the characteristic dependence on the atomic mass number A^2 that results in an increased differential recoil event rate for heavier target nuclei (coherent enhancement). The lack of coherent enhancement in the SD cross section results in typically lower differential recoil event rates than in the SI case and therefore weaker exclusion limits for σ_p^{SD} than for σ_p^{SI}. The limits for the SI cross section are typically presented in the $(m_\chi,\,\sigma_p^{\mathrm{SI}})$ plane as we shall see.

5.4.2 LHC and direct DM detection bounds on the CMSSM

In what follows I report my (and my collaborators') contribution to the global effort that, in the early years of this decade, was undertaken to constrain models on new physics with a variety of experimental data from the LHC and DM searches. One of these models is the Constrained MSSM (CMSSM).

The CMSSM was considered for many years the standard bearer of SUSY models in light of its reasonable assumptions on the transmission of supersymmetry breaking – via gravitational interactions at the scale of Grand Unification (GUT scale) – and for its limited number of free parameters.[1] In Ref. [H1] we showed that, by applying simultaneously and in a rigorous statistical approach the global set of experimental constraints available at the time one could exclude the most natural region of the parameter space of the CMSSM at the 95% C.L. The applied data included the measurement of the DM relic density, Eq. (2), the 2011 7 TeV Run of the LHC, the first 100 live days of the XENON 100 underground DM experiment, the anomalous magnetic moment of the muon, a large number of flavor and precision observables, data from indirect searches for DM in diffuse gamma rays from dwarf Spheroidal satellite galaxies (dSphs) of the Milky Way, and data from DM searches in the neutrino telescope IceCube.

To see how the data constrain natural regions of the parameter space, let us start by considering the 1-loop improved Higgs field potential, $V = \overline{M}^2\,|h|^2 + \bar{\lambda}\,|h|^4$, expressed in terms of the Higgs doublet field h of the SM, loop-corrected effective mass term $\overline{M}^2$, and quartic coupling $\bar{\lambda}$. The Higgs

[1] We remind the reader that the CMSSM has 4 free parameters: m_0, the universal soft SUSY-breaking scalar mass at the GUT scale; $m_{1/2}$, the universal GUT-scale gaugino mass; A_0, the universal GUT-scale soft trilinear coupling; and $\tan\beta$, the ratio of the Higgs doublets' vacuum expectation values. Plus one selects the sign of the superpotential Higgs mass parameter μ.

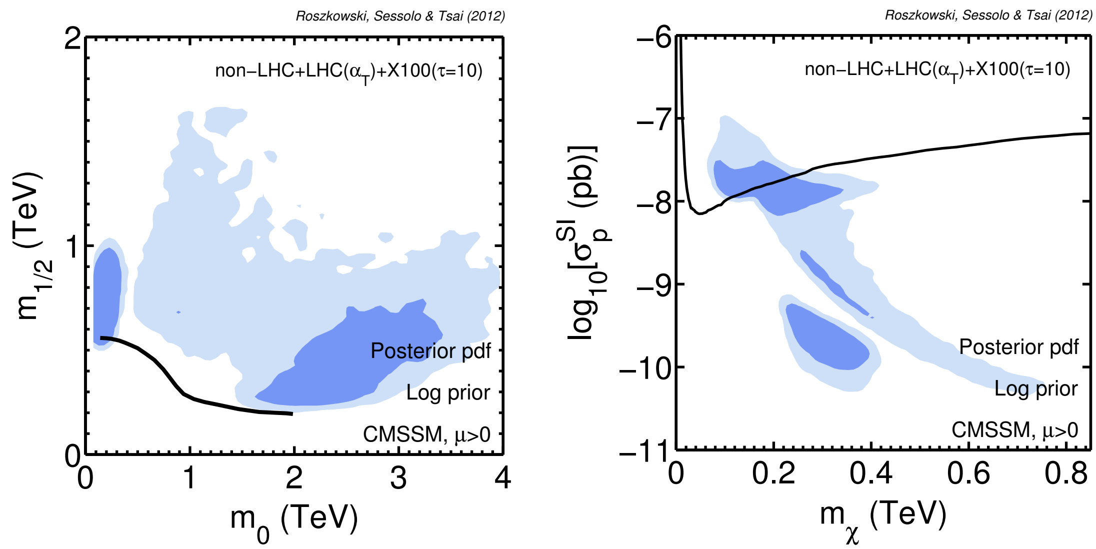

(a) (b)

Figure 1: (a) The 68% (dark blue) and 95% (light blue) credible regions of the marginalized 2D posterior pdf in the $(m_0,\, m_{1/2})$ plane of the CMSSM (ca. 2011). Black solid line shows the 95% C.L. upper bound from events with jets and missing energy at the LHC, included in the likelihood function. (b) The corresponding marginalized posterior pdf in the $(m_\chi,\, \sigma_p^{\mathrm{SI}})$ plane. Black solid line shows the 90% C.L. upper bound from a direct DM search at XENON 100. Both panels are taken from [H1].

boson mass is then defined as

$$m_h^2 \equiv -2\,\overline{M}^2 = m_{h,\mathrm{tree}}^2 + \delta m_h^2\,, \tag{9}$$

where δm_h^2 receives corrections from the fields of the eventually present UV completion. In the MSSM these corrections scale with the typical soft SUSY-breaking mass, M_{SUSY},

$$\delta m_h^2 \sim \frac{3y_t^2}{4\pi^2}\, M_{\mathrm{SUSY}}^2 \log\left(\frac{\Lambda}{\mathrm{TeV}}\right), \tag{10}$$

where y_t is the top quark Yukawa coupling and Λ a generic logarithmic cut-off scale. Scenarios are defined as natural if they do not involve a large cancellation between the tree level and loop corrections to the Higgs mass. As such, they are thought to require a typical superpartner mass $M_{\mathrm{SUSY}} \lesssim 1\,\mathrm{TeV}$.

In Fig. 1(a) we show a plot, taken from [H1], of the marginalized posterior probability density function (pdf) – which gives a measure of the Bayesian probability of the model's parameter space regions once the experimental constraints listed above are incorporated into a likelihood function – in the CMSSM, in the plane of the universal gaugino mass, $m_{1/2}$, versus the universal sfermion mass, m_0. Prior probability, encoded here as a logarithmic distribution, assigns equal statistical weight to equal logarithmic mass intervals. As the plot shows, the regions characterized by the highest probability (in dark blue) are also the most natural ones: either the sfermion mass, parameterized by m_0, or the gaugino mass, parameterized by $m_{1/2}$, preferably lie in the sub-TeV range.

Before proceeding to describe the impact of separate constraints on the parameter space, it is important to remind the reader that, typically, in the MSSM the DM particle is the lightest SUSY particle (LSP), whose stability is protected by a discrete symmetry called R-parity. In most realistic cases the LSP is the lightest neutralino (or, simply, the neutralino), which we indicate in the text as χ. This is a Majorana fermion mass eigenstate emerging, after EWSB, from the diagonalization of the mass matrix of four electrically and color-neutral SUSY states (see [21] for a comprehensive review). Two of these particles are gauginos, fermionic superpartners of the SM gauge bosons. The *bino*, in particular, is the partner of the $\mathrm{U}(1)_Y$ gauge boson, while the *wino* is the partner of the electrically neutral $\mathrm{SU}(2)_L$ gauge boson. The other two states are neutral *higgsinos*, which belong to a vector-like pair of Higgs doublet superfields.

At the tree level, the neutralino mass matrix takes the well-known form

$$\mathbf{M}_\chi = \begin{bmatrix} M_1 & 0 & -\frac{g' v_d}{\sqrt{2}} & \frac{g' v_u}{\sqrt{2}} \\ 0 & M_2 & \frac{g v_d}{\sqrt{2}} & -\frac{g v_u}{\sqrt{2}} \\ -\frac{g' v_d}{\sqrt{2}} & \frac{g v_d}{\sqrt{2}} & 0 & -\mu \\ \frac{g' v_u}{\sqrt{2}} & -\frac{g v_u}{\sqrt{2}} & -\mu & 0 \end{bmatrix}, \tag{11}$$

where g and g' are $\mathrm{SU}(2)_L$ and $\mathrm{U}(1)_Y$ gauge couplings, respectively, v_u and v_d are the vacuum expectation values (vev) of the neutral components of the scalar Higgs doublets (with the convention $v \equiv (v_u^2 + v_d^2)^{1/2} = 174\,\mathrm{GeV}$), M_1 and M_2 are the soft SUSY-breaking bare masses of the bino and wino, respectively, and μ is the vector-like mass parameter of the Higgs doublet superfields.

While it is the mass eigenstates that are the physical states, they can be dominated by some gauge eigenstates, a fact that allows one to make convenient approximations. In the limit where one among M_1, M_2, and μ is much smaller than the other parameters, the lowest eigenvalue approximately coincides with the lightest of these masses. In other words, $m_\chi \approx M_1$ when $M_1 \ll M_2, \mu$, and so on for interchanging orders. When two or more masses are instead comparable, mixing effects come into play and can change the phenomenology.

Returning to the two panels of Fig. 1 then, one can see the interplay of widely different experiments at work. In Fig. 1(a), the 2011 LHC bound, included in the likelihood function (but also shown indicatively as a solid black line) is shown to bite significantly into the high-probability region at very small m_0 and larger $m_{1/2}$, leaving instead the region at large m_0 and small $m_{1/2}$ almost untouched.

However, the 68% – 95% credible region at large m_0 and small $m_{1/2}$ is characterized by specific DM features. In fact, when imposing GUT-scale boundary conditions with scalar masses much larger than gauginos', one observes that renormalization group effects lead to $\mu \approx M_1$ ($\approx 100\mathrm{s}\,\mathrm{GeV}$) at the EWSB scale ("focus point" behavior). The DM is thus a neutralino with large mixing of bino and higgsino, characterized by large values of the spin-independent elastic scattering cross section, $\sigma_p^{\mathrm{SI}} \approx 10^{-8}\,\mathrm{pb}$. In Fig. 1(b) the posterior pdf is projected to the typical plane relevant for direct DM searches, that of σ_p^{SI} versus the neutralino mass. One can see that the XENON 100 upper bound, shown as a black solid line, bites deeply into this area of the parameter space, thus completing the siege on all of the natural regions.

The overall consequence, which has been shown after the first run of the LHC to similarly apply to virtually all of the mentioned new physics scenarios (and is thus not just restricted to the CMSSM), is that the low fine-tuning prejudice is of no help in predicting the mass and properties of any new particles. As such, it should be relinquished in favor of an approach that relies more solidly on the experimental data we possess.

5.5 Higgs mass measurement to the rescue

On July 4th, 2012, the discovery of the Higgs boson was announced at CERN by CMS and ATLAS. The last missing brick in the SM edifice had been finally placed, and we learned that the mass of the Higgs boson is $\sim 125\,\text{GeV}$.

While in the SM one does not gain particular insight by knowing the exact value of the Higgs boson mass – as this is essentially a free parameter that can take any value between the W, Z boson mass scale and a rough unitarity upper bound of $\sim 600\,\text{GeV}$ – in the MSSM the fact that $m_h = 125\,\text{GeV}$ has wide implications for the typical scale of the superpartners, M_{SUSY}.

Be recalling the 1-loop corrected Higgs mass, Eq. (9), we can use the minimization condition of the Higgs potential to write, in the limit where $v_u \gg v_d$,

$$\begin{aligned} m_h^2 &= -2\,\overline{M}^2 \\ &= 4\,\bar{\lambda}\,v^2 \\ &= 4\left(\frac{g'^2+g^2}{8}+\lambda_{\text{1-loop}}\right)v^2 \\ &\approx m_Z^2+\frac{3m_t^4}{4\pi^2v^2}\ln\left(\frac{M_{\text{SUSY}}^2}{m_t^2}\right)\,, \end{aligned} \tag{12}$$

where the third line is obtained by expanding $\bar{\lambda} = \lambda_{\text{tree}} + \lambda_{\text{1-loop}}$, we have used $2\,m_Z^2 = (g^2 + g'^2)\,v^2$ in the fourth line, and m_t is the top quark mass. I have assumed for simplicity that scalar top mixing terms can be neglected.

One can immediately see that the difference between the Higgs mass and Z boson mass, at about $125\,\text{GeV}$ and $91\,\text{GeV}$ respectively, provides a rough estimate of the size of M_{SUSY}. This estimate is not trivial, as one should use the fully re-summed renormalization-group improved scalar potential [22], and expectations depend strongly on parameters not shown in Eq. (12), like Higgs vev ratio $\tan\beta$ and trilinear coupling A_t. Moreover, because of the logarithmic dependence on M_{SUSY}, a theoretical uncertainty of a few GeV on the calculation of m_h can affect the value of M_{SUSY} by orders of magnitude. However, all sensible estimates have concluded that the mass of the Higgs boson at $125\,\text{GeV}$ implies typical values for M_{SUSY} in the 5 to few tens of TeV. In other words, when it comes to the MSSM the only genuine measured quantity that has emerged from the LHC pushes the spectrum away from the naive expectations of naturalness discussed in Sec. 5.4.

In Ref. [H2] my collaborators and I investigated the implications the newly discovered, at the time, Higgs boson had on SUSY parameter space and, in particular, DM. In Fig. 2(a) I show the marginalized 2D posterior pdf in the $(m_0,\ m_{1/2})$ plane of the CMSSM, where we applied to the likelihood function (an updated version of) all of the constraints described in Sec. 5.4, plus the mass of the Higgs boson at $125\,\text{GeV}$. The plot should be compared to Fig. 1(a).

By and large, the mass of the Higgs boson pushes now the high-probability region of the model in the regime of multi-TeV m_0 and $m_{1/2}$, as one could expect from our discussion following Eq. (12). Note, importantly, that the large credible region at the center of Fig. 2(a) is situated far away from the direct LHC lower bound from searches with jets and missing energy (dashed red line), and most likely also beyond any foreseeable high-luminosity reach. In other words the measured Higgs boson data, in contrast to vague and rather subjective expecations of naturalness, tells us we should not be surprised by the null results in direct searches for MSSM states at the LHC.

But what are the implications for neutralino DM searches? In Fig. 2(b) I project the marginalized 2D posterior pdf to the $(m_\chi,\ \sigma_p^{\text{SI}})$ plane. The plot should be compared to Fig. 1(b). Note the

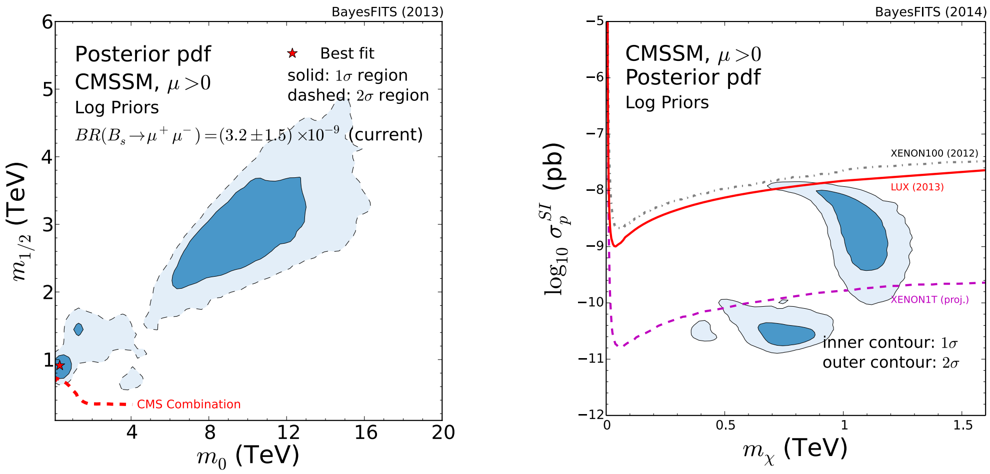

(a) (b)

Figure 2: (a) Marginalized 2D posterior pdf in the (m_0, $m_{1/2}$) plane of the CMSSM after the discovery of the Higgs boson (ca. 2013). The 68% credible regions are shown in dark blue, and the 95% credible regions in light blue. The dashed red line shows the CMS combined 95% C.L. exclusion bound [23]. The plot is taken from [H2]. (b) Marginalized 2D posterior pdf in the (m_χ, $\sigma_p^{\rm SI}$) plane for the CMSSM constrained by the mass of the Higgs boson, relic DM density, and experiments described in the text. Red solid line shows the 2013 LUX 90% C.L. exclusion bound [24] and dashed magenta line shows the projected 2-year sensitivity of XENON-1T. The plot is taken from [H3].

emergence of a large credibility regions at about $m_\chi \approx 1.1\,\text{TeV}$, which was not present in Fig. 1(b). In that area the neutralino DM candidate is a nearly pure higgsino, obtained by diagonalizing matrix (11) in the limit $\mu \approx 1\,\text{TeV} \ll M_{1,2} \approx m_{1/2}$. A $\sim 1\,\text{TeV}$ higgsino naturally leads to the correct relic density by means of its gauge quantum numbers, and is thus a very good candidate for the DM in the Universe. A higgsino much lighter than $1\,\text{TeV}$, on the other hand, leads to $\Omega_\chi h^2 \ll 0.12$, and thus requires one to assume the existence of an additional DM component, for example an axion.

5.6 Constraints and prospects for detection of neutralino dark matter

In Refs. [H3] and [H4] my collaborators and I investigated in exhaustive detail the experimental bounds and prospects for detection of neutralino DM in direct underground searches, indirect astrophysical signatures, and at the LHC, paying particular attention to the most promising candidate of the lot, the $\sim 1\,\text{TeV}$ higgsino, which, as I have just explained, emerges quite naturally as soon as the mass of the Higgs boson is incorporated into the likelihood function. Note that the properties and up-to-date constraints and prospects for detection of higgsinos of any mass value, thus including light higgsinos with $\Omega_\chi h^2 \ll 0.12$, were then summarized systematically in the invited review [H5].

As Fig. 2(b) shows, the $\sim 1\,\text{TeV}$ higgsino DM particle of the CMSSM enjoys enticing prospects for a timely detection in tonne-scale underground Xenon experiments, as its spin-independent scattering cross section is small enough to have escaped the current experimental bounds, but large enough to fall squarely within the reach of multi-tonne detectors.

On the other hand, low energy SUSY is a very broad framework, able to accommodate several

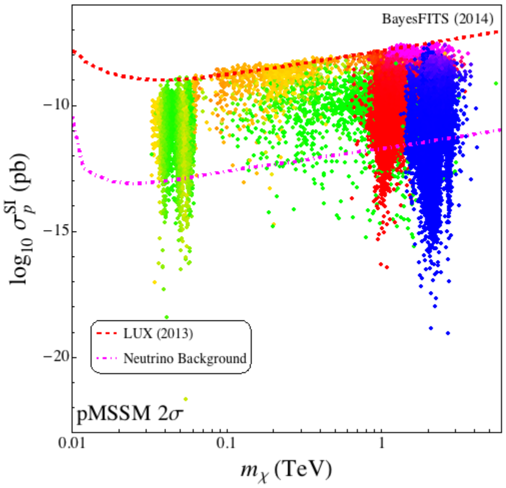

Figure 3: The parameter space of the pMSSM with $\Omega_\chi h^2 \approx 0.12$ in the $(m_\chi,\, \sigma_p^{\rm SI})$ plane. Points in green are characterized by a nearly pure bino composition of the neutralino; points in red are nearly pure higgsino; and points in blue are nearly pure wino. Bino/higgsino admixtures are shown in gold, wino/higgsino in magenta, and wino/bino in cyan. Dashed red line gives LUX direct detection bound (ca. 2013), and dot-dashed magenta line marks the onset of the irreducible atmospheric and solar neutrino background. Plot taken from [H4].

possibilities for the spectrum of superpartners. As SUSY must be broken in a hidden sector, little is known about the most likely mass pattern for the supersymmetric particles, and one must rely on reasonable assumptions driven by theory considerations. Thus, in order to analyze DM signatures in a general and model-independent SUSY scenario we analyzed in Ref. [H4] the DM issue in the phenomenological MSSM (pMSSM).

The pMSSM is the most general parametrization of the MSSM, based only on assumptions of Minimal Flavor Violation, R-parity conservation, and a level of CP violation not exceeding that of the SM. All popular SUSY scenarios with DM can be described in this framework by choosing appropriate boundary conditions. Since the number of free parameters in the pMSSM remains quite large, there is no real issue in fitting all the constraints belonging to the standard set described above. In particular, $\Omega_\chi h^2 \approx 0.12$ – in addition to all relevant collider constraints – can be fairly easily satisfied in different parts of the parameter space for different neutralino WIMP compositions.

I present in Fig. 3 the $2\,\sigma$ region in the $(m_\chi,\, \sigma_p^{\rm SI})$ plane of the pMSSM, emerging from the profile likelihood test statistics. The neutralino of the points in green is a nearly pure bino; for the points in red, it is a nearly pure higgsino (at $\sim 1\,$TeV); and for the points in blue it is a nearly pure wino, which yields the correct $\Omega_\chi h^2$ at larger mass scales. Bino/higgsino admixtures are shown in gold, wino/higgsino in magenta, and wino/bino in cyan. Note that in the pMSSM there is ample space for parameter space regions characterized by a very small $\sigma_p^{\rm SI}$, even below the onset of the irreducible atmospheric and diffuse supernova neutrino background (dot-dashed magenta line), which marks roughly the maximum reachable sensitivity in underground detectors with current technology.

In Ref. [H4] we showed that, particularly for these difficult-to-reach regions of the parameter space in the 1-to-several TeV mass range characterized by very low $\sigma_p^{\rm SI}$, the best prospects for detection might be provided by indirect searches for DM with γ-ray telescopes. In particular, by the approved Cherenkov Telescope Array (CTA) [25].

In collaboration with the CTA consortium we calculated the reach of CTA, in observations of

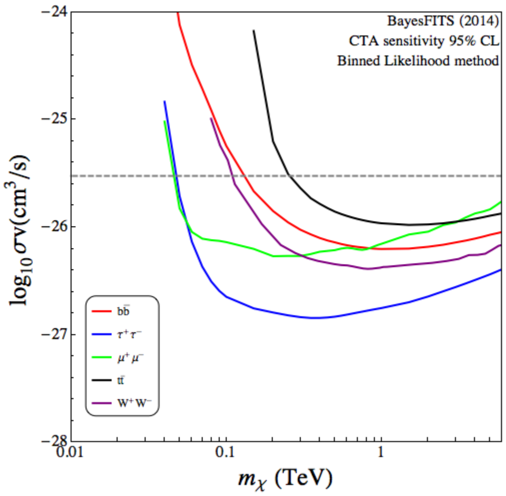

Figure 4: 95% C.L. CTA projected limits derived for the specific final states most commonly found in the pMSSM with the binned likelihood of Eq. (13) for the Einasto profile. Taken from [H4].

the Galactic Center, for the present day DM pair-annihilation cross section times velocity, σv, of particles with mass in the TeV regime. The reach of CTA in σv was calculated by means of a binned Poisson likelihood function, taking into account a detailed Monte-Carlo simulation of the cosmic-ray background and detector energy resolution. For each energy bin, i, the expected number of counts from DM annihilation reads

$$N_i^{\mathrm{ann}} = t_{\mathrm{obs}} \cdot J \cdot \frac{\sigma v}{8\pi m_\chi^2} \int_{\Delta E_i} dE \left(\frac{1}{\sqrt{2\pi\delta(E)^2}} \int_{26\,\mathrm{GeV}}^{m_\chi} d\bar{E} \frac{dN_\gamma(\bar{E})}{d\bar{E}} A_{\mathrm{eff}}(\bar{E}) e^{-\frac{(E-\bar{E})^2}{2\delta(E)^2}} \right), \tag{13}$$

where A_{eff} is the effective area of the detector, $\delta(E)$ is the energy resolution, both of them provided to us by the CTA Collaboration, dN_γ/dE is the diffuse gamma-ray spectrum for a specific annihilation final state, and J is the J-factor, which depends on the DM halo profile of the Milky Way (either Einasto or NFW). We considered a realistic observation time, $t_{\mathrm{obs}} = 500$ h.

The obtained projected limits are shown in Fig. 4 for the different annihilation final states listed in the legend. As WIMPs with mass in the TeV regime most often belong to non-trivial representations of the $\mathrm{SU}(2)_L$ group (as is the case, for example, of the *doublet* higgsino and the *adjoint triplet* wino) they preferentially annihilate into WW or ZZ, and their present day annihilation cross section does not drop much below the thermal relic expectation, shown in Fig. 4 with a dashed black line. Thus, CTA will prove to be an indispensable instrument to probe ranges of SUSY-model parameters that would otherwise be entirely out of reach by other direct means.

To highlight the idea of complementarity, we show in Fig. 5(a) the reach of CTA with 500 h of observation of the Galactic Center, compared to the reach of 1-tonne detectors in the (m_χ, σ_p^{SI}) plane. The color code is explained in the caption. In Fig. 5(b) we present the equivalent picture in the (m_χ, σ_p^{SD}) plane, compared to the estimated IceCube reach. And finally, we show in Fig. 5(c) the reach of CTA compared to the present limits on the stop mass, $m_{\tilde{t}_1}$, obtained in simplified models at the LHC. Figure 5 is taken from [H4]. Improvements in the LHC limits are not expected to have any effect on the sensitivity of CTA. Indeed, CTA remains sensitive to spectra where the gluinos and squarks lie well beyond the reach of present and future colliders.

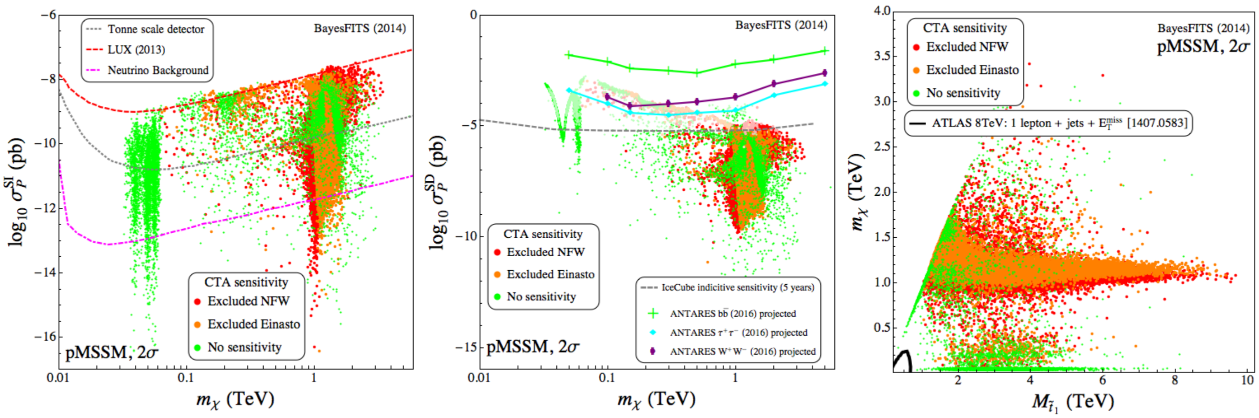

(a) (b) (c)

Figure 5: (a) The sensitivity of CTA 500 h Galactic Center observation in the (m_χ, σ_p^{SI}) plane of the pMSSM, for two choices of halo profile: NFW (red points), or Einasto (red+orange points). The approximate projected sensitivity of 1-tonne detectors is shown as a dotted gray line. The onset of the atmospheric and diffuse supernova neutrino background is shown with a dot-dashed magenta line. (b) The sensitivity of CTA to the pMSSM in the (m_χ, σ_p^{SD}) plane. Lighter shaded points are within the projected sensitivity of IceCube/DeepCore. The dashed gray line is indicative of IceCube's future sensitivity. (c) Sensitivity of CTA in the ($m_{\tilde{t}_1}$, m_χ) plane. The thick black line shows the approximate LHC lower bound on stop/neutralino masses. All figures are taken from [H4].

5.7 Interlude: WIMP reconstruction from direct detection and gamma rays

Before moving on to investigate the prospects for detection of some popular WIMP models not based on supersymmetry, I will briefly digress to consider what information about WIMP properties one could realistically derive in case a real DM signal is actually recorded in either direct detection or in gamma ray experiments, or – even better – in both.

Once one day a genuine DM signal is observed, we will enter into a new era of reconstructing WIMP properties from experimental data. A number of theoretical studies have been conducted to test the quality of a putative post-discovery reconstruction in direct detection experiments depending on the DM mass, respective cross section and target material (for a review see [26]). In particular, it has been pointed out that due to diminishing differences between recoil spectra for a larger DM mass, direct detection signal analysis can strongly constrain DM properties only for $m_\chi \lesssim 100$ GeV and for the values of σ_p^{SI} not far below the current limits given realistic assumptions about achievable exposures. For larger DM mass one typically obtains a $\sigma_p^{\mathrm{SI}}/m_\chi \sim$ const degeneracy.

However, my collaborators and I showed in Ref. [H6] that this can be partially overcome by a possible complementarity between direct and indirect detection strategies, provided, of course, that a DM-induced signal is found in both types of experiments. The idea hinges heavily on the construction of global likelihood functions that incorporate signals from different experiments.

In Fig. 6(a) I present the interplay between the underground XENON-1T detector [27] and two indirect detection experiments: CTA, based on the likelihood function described in Sec. 5.6 and Fermi-LAT [28] (for which I assume 15 years of exposure and 46 dSphs). As can be seen, an improved mass reconstruction in the indirect experiments allows one to strongly constrain σ_p^{SI} which remains unconstrained from above using direct detection data alone.

For a low DM mass a good reconstruction of m_χ in direct detection can help interpret the

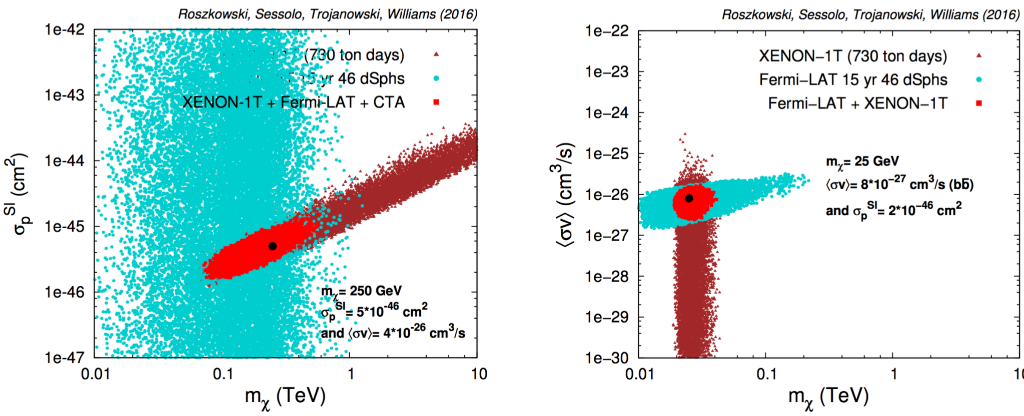

(a) (b)

Figure 6: (a) Comparison of XENON-1T and CTA + Fermi-LAT experiments in reconstructing the DM properties for the benchmark point with $m_\chi = 250\,\mathrm{GeV}$ and $\sigma_p^{\mathrm{SI}} = 5 \times 10^{-46}\,\mathrm{cm}^2$, while the annihilation cross section is equal to $\sigma v = 4 \times 10^{-26}\,\mathrm{cm}^3/\mathrm{s}$ for a pure $b\bar{b}$ final state. The brown region corresponds to 2σ reconstructed region for only XENON-1T simulated data, the light blue one for Fermi-LAT data (assuming 15 years of exposure and 46 dSphs in the stacked analysis), while the red region was obtained for XENON-1T+CTA+Fermi-LAT joint analysis. (b) Similar to (a), but for the benchmark point defined by $m_\chi = 25\,\mathrm{GeV}$, $\sigma_p^{\mathrm{SI}} = 2 \times 10^{-46}\,\mathrm{cm}^2$, $\sigma v = 8 \times 10^{-27}\,\mathrm{cm}^3/\mathrm{s}$ and pure $b\bar{b}$ annihilation final state. Light blue region corresponds to the the Fermi-LAT reconstruction, while the brown one to XENON-1T. The combined analysis leads to improved reconstruction of σv as indicated by the red region. Both figures are taken from [H6].

results of indirect detection searches. This is because it is difficult to distinguish among different DM scenarios based on results from indirect detection only, due to the a priori unknown nature of the annihilation final state and the lack of characteristic spectral features for typical final states channels, *e.g.*, $b\bar{b}$ or $\tau^+\tau^-$. However, different annihilation final states that provide a good fit to the same signal observed in indirect detection are often associated with different m_χ and σv. Hence, improved DM mass reconstruction in direct detection experiments could help in better discriminating among various annihilation final states and, eventually, constrain the annihilation cross section. I illustrate this in Fig. 6(b). As can be seen the DM mass reconstruction in Fermi-LAT is limited and it is a consequence of the aforementioned degeneracy in annihilation spectra. On the other hand, a direct measurement of a WIMP signal, which is obviously not sensitive to σv, helps reconstruct m_χ. As a result also the annihilation cross section that fits to the assumed signal from the benchmark point is constrained better. The reconstructed value of the annihilation cross section could then be mapped into the values of the DM relic density upon additional general assumptions about the WIMP interactions or within the framework of specific models.

5.8 Simplified WIMP models at the LHC

The third classical strategy for WIMP dark matter searches, after direct detection in underground laboratories and indirect signatures from astrophysical phenomena, is to try and produce a neutral stable particle in high-energy colliders. Given the typical weak coupling and EWSB-scale mass range expected for the WIMP the LHC can provide in principle an optimal instrument for pursuing this experimental venue.

Once faced with the realization that electroweak naturalness did not provide an effective tool in the search for new physics, many in the particle physics community scaled down their ambitions and started advocating a simplified approach designed to squeeze out the most generic and model-independent information from the data, in the hope of deriving new guidelines from the bottom up. For example, some scenarios contemplated the realistic possibility that the WIMP is the only new field around the EWSB scale, while additional visible particles, of any type, are sitting beyond the ultimate reach of the LHC detector. In that case the detection strategy must involve the identification in the scattering event of one (or a few) isolated, highly energetic, object(s) from initial state radiation, accompanied by large missing momentum. The object recoiling against the produced invisible particles can be a jet, a gauge boson, or a lepton, so that searches of this typology are commonly referred to in the literature as *mono-X* (where X stands for "jet," "photon," etc.) and have generated a great amount of activity and excitement in recent years.

While the LHC mono-X search results have been recast in and applied to numerous models with weak and sub-weak interactions (they proved particularly useful in probing compressed spectra in SUSY) they have been thoroughly compared to the bounds from direct and indirect DM detection searches in two preferential frameworks: effective field theory (EFT) and simplified model spectra (SMS).

In the EFT framework (see, *e.g.*, [29]), which was predominantly used by the LHC collaborations for their interpretations of the results of Run 1, one derives bounds on the strength of several contact operators, which can be then employed for a comparison with the limits on σ_p^{SI} and σ_p^{SD} from direct detection searches and neutrino detectors. The EFT can in principle provide a good approximation as long as the interaction is mediated by particles with mass well above the collision energy. But at the center-of-mass energies typically probed in a collider environment it is often necessary to consider models defined in terms of renormalizable interactions. In SMS (see, *e.g.*, [30] for a review) one introduces simple renormalizable Lagrangians, characterized by a limited number of free parameters, like the couplings of the DM to the visible sector, or the mass of the particles assumed to mediate the interaction between the DM and the partons in the nucleons. This and the next section will be dedicated to my work in the context of SMS.

Because of their reduced number of parameters, the most common SMS are not intrinsically equipped to capture some of the interesting phenomenology of more realistic theoretical DM models (for example the SUSY-based models treated in Secs. 5.4-5.6). In scenarios endowed with a rich spectrum of particles, in fact, several effects can arise which are missed in the most simple SMS, like long decay chains, or the well known presence of "blind spots," pockets of the parameter space where interference between different diagrams or a small effective coupling of the DM particle to the SM can lead to a suppressed cross section for direct detection. Moreover, with a larger number of particles with differentiated properties one can make a more effective use of the complementarity of different experimental strategies, which can be employed in combination.

In Ref. [H7] my collaborators and I gave a detailed look at the detection issues arising in cases when one moves just one step beyond the SMS approach, *i.e.* when one tries to build models that are halfway in between those SMS characterized by just one type of mediator and interaction mechanism, and a UV complete model. We combined existing SMS in pairs, with the goal to somewhat mimic the behavior of a developed UV theory without at the same time drastically increasing the number of parameters, or including the full spectrum of a specific model.

For example one can consider the combination of two popular simplified models: the Z' portal and the Higgs portal. In the Z' portal, the mediator between a hypothetical Dirac fermion gauge-singlet DM particle, which we call with some redundancy χ, and the SM is a leptophobic Z' boson. The new mediator is assumed to have negligible mixing with the Z boson of the SM, and to not couple to the SM leptons, so that one can easily evade the strong limits from di-lepton resonances at the LHC.

The interaction terms relative to DM detection at the LHC and in underground detectors are

$$\mathcal{L} \supset Z'_\mu \bar{\chi}\gamma^\mu (g_\chi^V - g_\chi^A \gamma_5)\chi + \sum_i Z'_\mu \bar{q}_i \gamma^\mu (g_q^V - g_q^A \gamma_5) q_i \,, \tag{14}$$

where the index i runs over the quarks and we have universal vector (axial-vector) quark couplings g_q^V (g_q^A). The corresponding vector and axial-vector couplings to the DM are g_χ^V and g_χ^A, respectively.

The Higgs portal features instead χ, the fermion DM singlet, coupled to a new singlet real scalar, s. The terms in the Lagrangian relevant to DM searches are

$$\mathcal{L} \supset -y_\chi \bar{\chi}\chi s - \mu_s s |\Phi|^2 - \lambda_s s^2 |\Phi|^2, \tag{15}$$

where y_χ is the Yukawa coupling between the DM and the singlet, and μ_s is a mass term that induces mixing between s and the SM Higgs doublet, Φ, that gives rise to the Higgs boson after EWSB.

The μ_s and λ_s Lagrangian terms produce an off-diagonal component in the (h, s) mass matrix, thus the mass matrix is diagonalized by a mixing matrix parametrized by a mixing angle θ. In general we will identify the lightest scalar with the observed SM-like Higgs. Higgs physics measurement, electroweak precision tests, and vacuum stability then constrain $|\sin\theta|$.

After diagonalization the relevant terms in the Lagrangian (15) for DM phenomenology are

$$\mathcal{L} \supset -y_\chi \left(h_{\rm SM}\sin\theta + H\cos\theta\right)\bar{\chi}\chi - \frac{1}{\sqrt{2}}\left(h_{\rm SM}\cos\theta - H\sin\theta\right)\sum_f y_f \bar{f} f \,, \tag{16}$$

where y_f are the SM Yukawa couplings and $f, \bar{f}$ SM fermions. This results in the presence of a heavy scalar mediator, H, as well as the SM Higgs, h_{SM}, that couple the DM to the quarks.

When both the Z' and Higgs portal are present the contribution to the amplitude for $\sigma_p^{\rm SI}$ reads

$$f_p \approx \frac{y_\chi \sin 2\theta}{4\, m_{h_{\rm SM}}^2}\left(1 - \frac{m_{h_{\rm SM}^2}}{m_H^2}\right)\frac{m_p}{v}\left(\sum_{q=u,d,s} f_{Tq} + \frac{2}{9} f_{TG}\right) + \frac{3}{2}\frac{g_\chi^V g_q^V}{m_{Z'}^2} \,, \tag{17}$$

where m_p is the nucleon mass, and f_{Tq} and f_{TG} are the hadronic matrix elements defined for example in [21].

If $y_\chi > 0$, $m_H \gg m_{h_{\rm SM}}$, and $g_\chi^V = g_q^V$, destructive interference between the terms in Eq. (17) does not take place. On the other hand, if $y_\chi < 0$, or if it is positive but $g_\chi^V = -g_q^V$, the diagrams corresponding to the Z' and Higgs portal interfere destructively and $\sigma_p^{\rm SI}$ becomes suppressed, as can be inferred from Eq. (17). The effects of this cancellation are shown for a benchmark point with $m_\chi = 10\,\text{GeV}$ in Fig. 7(a). The blind spot is in the plots a narrow diagonal region, over which the value of $\sigma_p^{\rm SI}$ visibly drops below the potential reach of tonne-scale detectors. The corresponding case for $m_\chi = 100\,\text{GeV}$ is shown in Fig. 7(b). Note how the interplay of mono-jet searches, searches for Z' resonances, and Higgs width measurements effectively constrain the parameters of the model, when the condition for a blind spot is satisfied.

Other cases analyzed in Ref. [H7] involved blind spots emerging from the combination of the two portal models described above with a model involving scalar t-channel mediators charged under color.

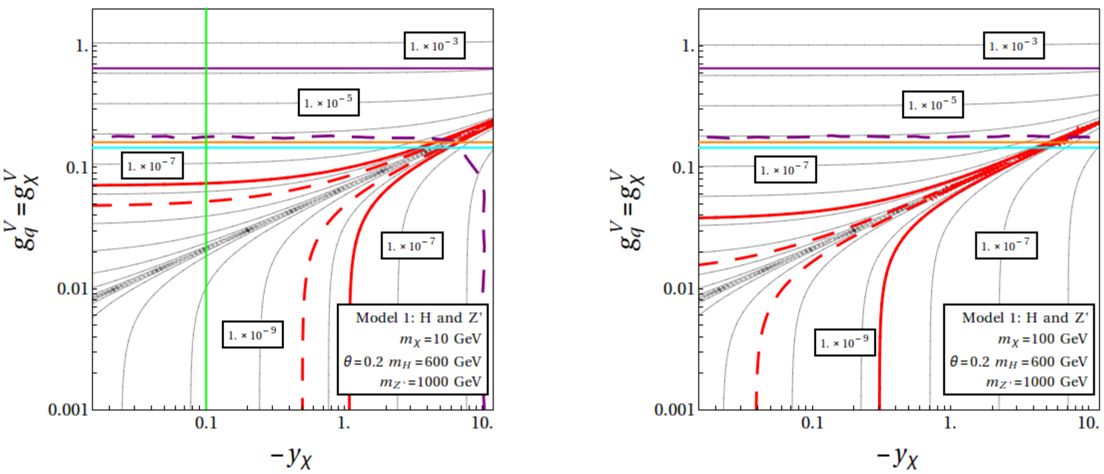

(a) (b)

Figure 7: (a) Spin-independent scattering cross section in pb in the $(y_\chi,\ g^V_{\chi/q})$ plane for a model combining Z' mediator and Higgs portal. We set $m_\chi = 10\,\text{GeV}$, $m_{Z'} = 1000\,\text{GeV}$, $\theta = 0.2$ and $m_H = 600\,\text{GeV}$. The solid red line represents the 90% C.L. upper bound from LUX and the dashed red line is the projected 2-yr limit for tonne-scale detectors. Solid purple line is the 95% C.L. upper bound from the 8 TeV mono-jet search at ATLAS. Dashed purple line is the projected limit from the mono-jet search at 14 TeV with $300\,\text{fb}^{-1}$. Solid orange line gives the upper limit from searches for heavy vector resonances in the di-top channel at 8 TeV, and the solid cyan line gives the equivalent limit in the $\bar{q}q$ search. Green solid line gives the upper limit from the invisible width of the Higgs boson in a CMS/ATLAS combined analysis (see [H7] and references to the experiments therein). (b) Same as (a) but $m_\chi = 100\,\text{GeV}$. Plots taken from [H7].

5.9 Simplified WIMP models and the muon $g-2$

Finally, still in the context of the SMS approach, in Ref. [H8] I looked at what information about the properties of WIMP DM can be inferred from existing experimental anomalies that might be the first manifestation of new physics waiting to be confirmed as soon as more data becomes available.

In particular, the anomalous magnetic moment of the muon, $(g-2)_\mu$, was measured at BNL several years ago [31], showing a discrepancy with the SM expectation that has since been widely interpreted as a hint for new physics not far from the EWSB scale. The discrepancy, $\delta\,(g-2)_\mu$, is estimated to be at the level of $\sim 3.5\,\sigma$, or $\delta\,(g-2)_\mu = (27.4 \pm 7.6) \times 10^{-10}$. The new Muon g-2 experiment at Fermilab [32], will improve the statistical precision of the measurement by a factor of four or so with respect to BNL. Additionally, just a few years after the Fermilab experiment, $(g-2)_\mu$ will also be measured at J-PARC [33], which is expected to reach a comparable sensitivity even if the experimental setup is different.

In Ref. [H8] we addressed the following question: in case a positive measurement of $\delta\,(g-2)_\mu$ is obtained with large significance at Fermilab, what information can we infer on the couplings, masses, and quantum numbers of the new particles involved in the process, provided we require that the same physics also yields the relic density of DM in the Universe. As the nature of DM constitutes one of the greatest mysteries in contemporary particle physics, it is enticing to entertain the idea that a positive measurement at Fermilab and J-PARC could open a window into the nature of the dark sector, possibly in conjunction with other experimental signatures. We showed that requiring the same physics to be responsible for the $(g-2)_\mu$ anomaly and DM leads to strong bounds on the allowed parameter space and introduces a series of complementary signatures, in particular at the high-luminosity LHC, in future electroweak precision experiments and, to a lesser extent, in DM direct detection searches.

We considered a set of scenarios in which both the DM and the lepton mediator can transform non-trivially under the $\mathrm{SU}(2)_L$ gauge group. The simplified models we constructed were based on the following requirements:

- The DM interacts with the muons through renormalizable couplings
- Interactions are CP conserving and invariant under the SM gauge group, $\mathrm{SU}(2)_L\times\mathrm{U}(1)_Y$
- Each model satisfies the constraints from perturbativity and unitarity
- The measurement of the relic abundance is an active constraint on the parameter space.

We considered several combinations of SMS with matter transforming under different representations of the gauge group: scalar singlets with fermion singlets, fermion doublets, or both. Scalar doublets, with fermion singlets, doublets, triplets, adjoint triplets, and combinations of those. I present here but one example of these constructions, but the interested reader can refer for all other combinations to Ref. [H8]. In all of the considered cases the DM particle emerged as one of the scalar fields, which could pair annihilate in the early Universe into a pair of Higgs bosons (Higgs portal) or a pair of muons (lepton portal).

The simplest of these SMS is constructed by extending the SM with a singlet real scalar field, s, and a pair of singlet vector-like fermion fields, E, E'. The parameters of the scalar potential are constrained by theoretical requirements, in order to guarantee that the electroweak vacuum is a global minimum. The parameters and constraints on the scalar potential can be found in [H8].

The model is then subject to the following constraints:

- LHC 13 TeV bounds from searches for leptons and missing E_T
- LHC 13 TeV mono-jet search bounds
- Electroweak precision constraints from the Z lineshape and asymmetry data at LEP and measurements of the muon lifetime and W mass
- Where applicable (portal couplings), direct detection constraints from LUX and XENON-1T.

In Fig. 8(a) I present a plot of the model's parameter space in the plane of the Yukawa coupling Y_S between the muon and the singlet states versus the DM mass. The parameter space allowed at $2\,\sigma$ (including a $\sim 10\%$ theory error) by the relic density is shown in cyan. The $(g-2)_\mu$ constraint is shown in dark blue and we do not impose at this stage any LHC or precision constraints.

Note that the relic abundance imposes a lower bound on the mass of the scalar particle, $m_s = m_{\mathrm{DM}} \gtrsim 40-50\,\mathrm{GeV}$, as the annihilation mechanism loses its efficiency when the spread between m_s and m_E is significant (recall that for the new fermions one has $m_E \gtrsim 100\,\mathrm{GeV}$ by LEP bounds). The parameter space allowed at $2\,\sigma$ by the combination of relic density and $(g-2)_\mu$ is shown in green. The $2\,\sigma$ region from the BNL measurement places an upper bound on the mass of the dark matter scalar, $m_{\mathrm{DM}} \lesssim 170-180\,\mathrm{GeV}$, beyond which one is forced to resort to non-perturbative values for the new Yukawa coupling Y_S, independently of the size of $m_E > m_{\mathrm{DM}}$.

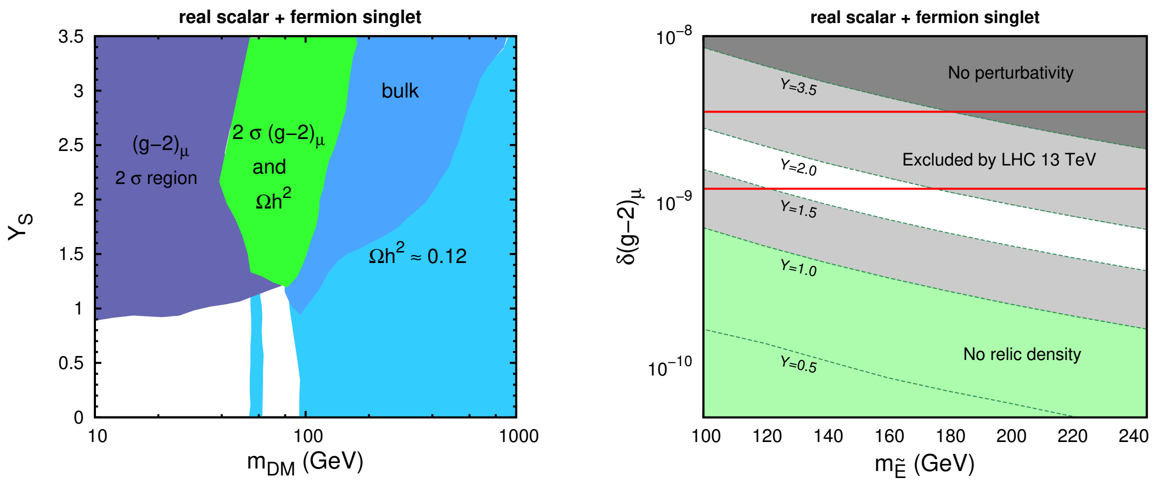

(a) (b)

Figure 8: (a) The $(m_{\rm DM}, Y_S)$ plane for Model 1 (real scalar field and VL fermion singlet). In cyan, the parameter space favored at 2σ by the relic density is shown, while the one favored by the $(g-2)_\mu$ measurement is shown in dark blue. Green region corresponds to those values of model parameters where both constraints are satisfied simultaneously. (b) Predictions for the mass of new fermions given the measurement of $\delta\,(g-2)_\mu$. The parameter space is strongly constrained by the LHC, with the exception of a narrow strip. The DM mass is fixed here at 80 GeV. Plots taken from [H8].

One can draw some predictions for future measurements of $(g-2)_\mu$ under the hypothesis that the anomaly measured at BNL will be confirmed and that the same underlying physics is responsible for the relic abundance of DM in the Universe. I show this in Fig. 8(b), where one can see that once the bounds from the LHC are computed, through a detailed numerical simulation whose details can be found in [H8], the surviving parameter space is confined to a very narrow strip, shown in white.

In the same note, we found that all models composed of one scalar and one pair of vector-like fermions, of any representation, were strongly constrained by multilepton plus missing E_T searches at the LHC. However, for both the real and complex singlet scalar, when singlet and doublet pairs of VL fermions were allowed to mix through interactions with the SM Higgs, the introduced source of chiral-symmetry violation, by being proportional to the mass of the heavy leptons, could boost $\delta\,(g-2)_\mu$. The anomaly could thus be accommodated for masses up to $\sim 3\,$TeV. The same effect, however, generates large contributions to the electroweak precision observables that, for the large fermion mixing, exclude part of the parameter space.

5.10 Summary and conclusions

A wide collection of data has proven beyond any reasonable doubt the existence of dark matter, which accounts for about 25% of the energy content of the Universe. The long-held paradigm is that the dark matter is composed of weakly interactive massive particles (WIMPs), which froze out of thermal equilibrium early after the Big Bang. In recent years, this so-called WIMP paradigm has been tested extensively through direct experiments in underground laboratories, indirect astrophysical searches, and in collider searches at the LHC. In this report of scientific goals I have provided a summary of my contribution to this collective investigative effort.

I made the point that, while all of the searches have so far given null results, they have also provided us with a great amount of information that can be used to direct new searches and probe regions of the parameter space that were previously unexplored. In particular, in the first part of this report I have described how the bounds from the LHC and Xenon underground detectors constrained the parameter space leading to solutions without fine tuning. However, the concept of "naturalness" itself is only vaguely defined and might have provided the wrong guidance. I showed that, when we instead rely on the experimental information that has become recently available, in the form for example of the measurement of the Higgs boson mass at the LHC, new candidates for dark matter might be expected, which will possibly require new instruments for a detection. I made the point that the better motivated of these candidates is, in my opinion, the $\sim 1\,\text{TeV}$ higgsino of low-scale supersymmetry.

In the second part of this report I have shown instead that a variety of different experimental strategies can be used in combination to obtain stringent bounds on the parameter space of many generic models of WIMP dark matter. These bounds provide predictions that are independent of any considered UV completion, but are correlated with a large number of complementary signatures emerging, for example, in low-energy flavor physics observables like the anomalous magnetic moment of the muon.

6 Other scientific achievements

6.1 Bibliometric data (as of September, 2018)

According to inSPIRE

number of papers: 24
number of citations: 822
number of citations without self-citations: 655
h-index (Hirsch index): 13
total impact factor (the sum of 5-year journal impact factors): 124

According to the Web of Science

number of papers: 25
number of citations: 496
number of citations without self-citations: 441
h-index (Hirsch index): 12

6.2 Other publications and their main results

6.2.1 After PhD

[P1] Kamila Kowalska, Enrico Maria Sessolo,
Gauge contribution to the $1/N_F$ *expansion of the Yukawa coupling beta function*,
JHEP **1804** (2018) 027 (arXiv:1712.06859).

We provided, for the first time in the literature, a closed analytical form for the gauge contribution to the beta function of a generic Yukawa coupling in the limit of large N_F, where N_F is the number of heavy vector-like fermions charged under an abelian or non-abelian gauge group. The resummed expression is finite and for the abelian case presents a pole at the same location as for the corresponding gauge beta function.

[P2] Leszek Roszkowski, Enrico Maria Sessolo, Sebastian Trojanowski,
WIMP dark matter candidates and searches - current status and future prospects,
Rept.Prog.Phys. **81** (2018) no.6, 066201 (arXiv:1707.06277).

We reviewed several current aspects of dark matter theory and experiment. We overviewed the current experimental status and briefly reviewed several possible particle candidates for a Weakly Interactive Massive Particle (WIMP) and dark matter recently considered in the literature. We paid particular attention to the lightest neutralino of supersymmetry as it remains the best motivated candidate for dark matter and also shows excellent detection prospects. Finally we briefly reviewed some alternative scenarios that can considerably alter properties and prospects for the detection of dark matter obtained within the standard thermal WIMP paradigm.

[P3] Arghya Choudhury, Luc Darmé, Leszek Roszkowski, Enrico Maria Sessolo, Sebastian Trojanowski,
Muon $g-2$ and related phenomenology in constrained vector-like extensions of the MSSM,
JHEP **1705** (2017) 072 (arXiv:1701.08778).

We analyzed two minimal supersymmetric constrained models with low-energy vector-like matter preserving gauge coupling unification. In one we add to the MSSM spectrum a pair $\mathbf{5}+\overline{\mathbf{5}}$ of SU(5), in the other a pair $\mathbf{10}+\overline{\mathbf{10}}$. We showed that the muon $g-2$ anomaly can be explained in these models while retaining perturbativity up to the unification scale, satisfying electroweak and flavor precision tests and current LHC data. We examined also some related phenomenological features of the models, including Higgs mass, fine-tuning, dark matter and several LHC signatures.

[P4] Kamila Kowalska, Enrico Maria Sessolo,
MSSM fits to the ATLAS 1 lepton excess,
Eur.Phys.J. **C77** (2017) no.2, 79 (arXiv:1611.01852).

We performed a SUSY fit to the (now disappeared) excesses over the Standard Model background observed in three bins of the ATLAS 1-lepton + (b-)jets + MET 2016 search. We found a few types of spectra fitting the emerging signal. The first class was characterized by the presence of one stop or stop and sbottoms with mass in the ballpark of 700 - 800 GeV and a neutralino LSP of mass around 400 GeV. In the second type of scenarios the stop, lightest chargino, sbottom, and the neutralino were at about or heavier than 650 GeV and the signal originated from cascade decays of squarks of the 1st and 2nd generation. For the best-fit scenarios we showed that the putative signal was also favored globally with respect to the background only hypothesis.

[P5] Mihailo Backović, Suchita Kulkarni, Alberto Mariotti, Enrico Maria Sessolo, Michael Spannowsky,
Cornering diphoton resonance models at the LHC,
JHEP **1608** (2016) 018 (arXiv:1605.07962).

We explored the ability of the high luminosity LHC to test models which could explain the (now disappeared) 750 GeV diphoton excess. We focused on a wide class of models where a 750 GeV singlet scalar coupled to Standard Model gauge bosons and quarks, as well as dark matter. Including both gluon and photon fusion production mechanisms, we showed that LHC searches in channels correlated with the diphoton signal would have been able to probe wide classes of diphoton models with 3000/fb of data.

[P6] Kamila Kowalska, Jacek Pawełczyk, Enrico Maria Sessolo,
Flavored gauge mediation in the Peccei-Quinn NMSSM,
JHEP **1512** (2015) 148 (arXiv:1508.04142).

We investigated a particular version of the Peccei-Quinn NMSSM characterized by an economical and rigidly hierarchical flavor structure and based on flavored gauge mediation and on some considerations inspired by string theory GUTs. One of the most important results of the study was to show that, despite requiring the unavoidable introduction of large scale superpotential and soft Lagrangian effective terms that are linear and quadratic in the singlet field, the model does not present fine-tuning levels higher than the ones present in the MSSM, contrary to what was commonly believed.

[P7] Kamila Kowalska, Leszek Roszkowski, Enrico Maria Sessolo, Andrew J. Williams,
GUT-inspired SUSY and the muon $g-2$ anomaly: prospects for LHC 14 TeV,
JHEP **1506** (2015) 020 (arXiv:1503.08219).

We considered the possibility that the muon $g-2$ anomaly find its origins in low energy supersymmetry (SUSY). We found that in the general MSSM the parameter space consistent with $g-2$ and correct dark matter relic density of the lightest neutralino easily evaded direct LHC limits on sparticle masses and lied to a large extent beyond future LHC sensitivity. But the situation was quite different in GUT-defined scenarios where input SUSY parameters were no longer independent. We analyzed to what extent the LHC could probe a broad class of GUT-inspired SUSY models with gaugino non-universality that were in agreement with the relic density, $g-2$, and the Higgs mass measurement. We performed a detailed numerical simulation of several searches for electroweakino and slepton production at the LHC and derived projections for the LHC 14 TeV run. We demonstrated that the parameter space would be basically fully explored within the sensitivity of the 14 TeV run with 300/fb.

[P8] Kamila Kowalska, Leszek Roszkowski, Enrico Maria Sessolo, Sebastian Trojanowski,
Low fine tuning in the MSSM with higgsino dark matter and unification constraints,
JHEP **1404** (2014) 166 (arXiv:1402.1328).

We examined the issue of fine tuning in the MSSM with GUT-scale boundary conditions. We analyzed several popular cases: the CMSSM, models with non-universal gaugino masses, and models with non-universal scalar masses. We showed that the mechanism of parameter-focusing along the RGE running is, for certain specific GUT-relations, very efficient in lowering the fine tuning of the scalar and gaugino sectors in the ~ 1 TeV higgsino region with respect to the case with universal masses.

[P9] Kamila Kowalska, Enrico Maria Sessolo,
Natural MSSM after the LHC 8 TeV run,
Phys.Rev. **D88** (2013) no.7, 075001 (arXiv:1307.5790).

We investigated the impact of direct LHC SUSY searches on the parameter space of three natural scenarios in the MSSM. In the first case the spectrum consisted of light stops, sbottoms, and Higgsino-like neutralinos. In the second case we considered an additional light gluino. Finally we studied a more complex spectrum comprising also light sleptons, wino-like chargino, and a bino-like neutralino. We simulated in detail three LHC searches: stop production at ATLAS with 20.7/fb, CMS 11.7/fb inclusive search for squarks and gluinos with the variable α_T, and CMS 9.2/fb electroweak production with 3 leptons in the final state. For each point in our scans we calculated the exclusion likelihood due to the individual searches and to their statistical combination. We found that points with acceptable levels of fine-tuning were for the most part already excluded by the LHC and including other constraints further reduced the overall naturalness of the considered scenarios.

[P10] Andrew Fowlie, Kamila Kowalska, Leszek Roszkowski, Enrico Maria Sessolo, Yue-Lin Sming Tsai,
Dark matter and collider signatures of the MSSM,
Phys.Rev. **D88** (2013) 5, 055012 (arXiv:1306.1567).

We performed a global statistical analysis of a parametrization of the MSSM with 9 free parameters defined at the SUSY scale, the p9MSSM. We confronted the model with a set of experimental constraints including measurement of the relic density from PLANCK, the discovery of the Higgs boson, LHC direct SUSY searches, the evidence for a Standard Model-like $\mathrm{BR}\left(\mathrm{B_s} \to \mu^+\mu^-\right)$, and the measurement of $\delta\left(g-2\right)_\mu$, plus a number of other electroweak and flavor physics constraints. We also performed a simulation of two LHC direct SUSY searches at $\sqrt{s} = 8$ TeV. We found that a neutralino mass consistent at 2σ with all the constraints was in the window $[200 - 500]$ GeV.

[P11] Kamila Kowalska, Shoaib Munir, Leszek Roszkowski, Enrico Maria Sessolo, Sebastian Trojanowski, Yue-Lin Sming Tsai,
The Constrained NMSSM with a 125 GeV Higgs boson – A global analysis,
Phys.Rev. **D87** (2013) 11, 115010 (arXiv:1211.1693).

We performed the first global analysis of the Constrained NMSSM that investigated the impact of the (at the time) recently discovered Higgs boson with a mass of around 125 GeV. Since in the framework of the NMSSM there exists two scalars that can be light, we considered three possible cases, assuming in turn that the discovered Higgs boson was the lightest Higgs boson of the model; the next-to-lightest Higgs boson; and a combination of both roughly degenerate in mass. We fond that, when a set of experimental constraints was applied, the first case showed strong CMSSM-like behavior. On the other hand, the second and the third cases were disfavored by the constraints from direct detection of dark matter and from the measurement of $\mathrm{BR}\left(\mathrm{B_s} \to \mu^+\mu^-\right)$.

[P12] Andrew Fowlie, Małgorzata Kazana, Kamila Kowalska, Shoaib Munir, Leszek Roszkowski, Enrico Maria Sessolo, Sebastian Trojanowski, Yue-Lin Sming Tsai,
The CMSSM Favoring New Territories: The Impact of New LHC Limits and a 125 GeV Higgs,
Phys.Rev. **D86** (2012) 075010 (arXiv:1206.0264).

In this study we performed one of the first ever global analyses of the Constrained MSSM to take into account the impact of a Higgs boson with a mass of around 125 GeV. We identified high posterior probability regions of the CMSSM parameters and found that the well-known focus-point region of the parameter space was disfavored by the Higgs boson mass measurement.

6.2.2 Before PhD

[B1] Vernon Barger, Jason Kumar, Danny Marfatia, Enrico Maria Sessolo,
Fermion WIMPless dark matter at DeepCore and IceCube,
Phys.Rev. **D81** (2010) 115010 (1004.4573).

We investigated the prospects for indirect detection of fermion WIMPless dark matter at the neutrino telescopes IceCube and DeepCore. The dark matter annihilating in the Sun was a hidden sector Majorana fermion that coupled through Yukawa couplings to a connector particle and a visible sector particle, and it exhibited only spin-dependent scattering with nuclei via couplings to first generation quarks. We considered cases where the annihilation products were taus, staus, or sneutrinos of the three generations. To evaluate the muon fluxes incident at the detector, we numerically propagated the neutrino spectra through the solar medium and to the Earth and accounted for the effects of neutrino oscillations, energy losses due to neutral- and charged-current interactions, and tau regeneration.

[B2] E. M. Sessolo, F. Tahir, D. W. McKay,
Multi-parameter approach to R-parity violating SUSY couplings,
Phys.Rev. **D79** (2009) 115010 (0903.0118).

We introduced and implemented a new, extended approach to placing bounds on trilinear R-parity violating couplings. We focused on a limited set of leptonic and semi-leptonic processes involving neutrinos, combining multidimensional plotting and cross-checking constraints from different experiments. This allowed us to explore new regions of parameter space and to relax a number of bounds given in the literature. We looked for qualitatively different results compared to those obtained previously using the assumption that a single coupling dominates the R-parity violating contributions to a process. By combining results from several experiments, we identified regions in parameter space where two or more parameters approach their maximally allowed values. In the same vein, we showed a circumstance where consistency between independent bounds on the same combinations of trilinear coupling parameters implied mass constraints among slepton or squark masses.

[B3] E. M. Sessolo, D. W. McKay,
Eikonal contributions to ultra high energy neutrino-nucleon cross sections in low-scale gravity models,
Phys.Lett. **B668** (2008) 396-403 (0803.3724).

We calculated low scale gravity effects on the cross section for neutrino-nucleon scattering at center of mass energies up to the Greisen-Zatsepin-Kuzmin scale, in the eikonal approximation. We compared the cases of an infinitely thin brane embedded in 5 compactified extra-dimensions, and of a brane with a physical tension that could be either 1 TeV or 10 TeV. The extra dimensional Planck scale was set at either 1 TeV or 2 TeV. We also compared our calculations with neutral-current SM calculations in the same energy range, and compared the thin-brane eikonal cross section to its saddle-point approximation. New physics effects enhance the cross section by orders of magnitude on average. They are quite sensitive to parameter choices, though much less sensitive to the number of extra dimensions.

References

[1] G. D'Amico, M. Kamionkowski, and K. Sigurdson, "Dark Matter Astrophysics," `arXiv:0907.1912 [astro-ph.CO]`.

[2] A. Del Popolo, "Nonbaryonic Dark Matter in Cosmology," *Int. J. Mod. Phys.* **D23** (2014) 1430005, `arXiv:1305.0456 [astro-ph.CO]`.

[3] F. Zwicky, "Die Rotverschiebung von extragalaktischen Nebeln," *Helv. Phys. Acta* **6** (1933) 110–127.

[4] V. C. Rubin and W. K. Ford, Jr., "Rotation of the Andromeda Nebula from a Spectroscopic Survey of Emission Regions," *Astrophys. J.* **159** (1970) 379–403.

[5] V. C. Rubin, N. Thonnard, and W. K. Ford, Jr., "Rotational properties of 21 SC galaxies with a large range of luminosities and radii, from NGC 4605 /R = 4kpc/ to UGC 2885 /R = 122 kpc/," *Astrophys. J.* **238** (1980) 471

[6] D. Clowe, M. Bradac, A. H. Gonzalez, M. Markevitch, S. W. Randall, C. Jones, and D. Zaritsky, "A direct empirical proof of the existence of dark matter," *Astrophys. J.* **648** (2006) L109–L113, `arXiv:astro-ph/0608407 [astro-ph]`.

[7] **Planck** Collaboration, P. A. R. Ade *et al.*, "Planck 2015 results. XIII. Cosmological parameters," *Astron. Astrophys.* **594** (2016) A13, `arXiv:1502.01589 [astro-ph.CO]`.

[8] M. Li, X.-D. Li, S. Wang, and Y. Wang, "Dark Energy," *Commun. Theor. Phys.* **56** (2011) 525–604, `arXiv:1103.5870 [astro-ph.CO]`.

[9] S. W. Randall, M. Markevitch, D. Clowe, A. H. Gonzalez, and M. Bradac, "Constraints on the Self-Interaction Cross-Section of Dark Matter from Numerical Simulations of the Merging Galaxy Cluster 1E 0657-56," *Astrophys. J.* **679** (2008) 1173–1180, `arXiv:0704.0261 [astro-ph]`.

[10] A. Del Popolo and M. Le Delliou, "Small scale problems of the ΛCDM model: a short review," *Galaxies* **5** no. 1, (2017) 17, `arXiv:1606.07790 [astro-ph.CO]`.

[11] M. Viel, G. D. Becker, J. S. Bolton, and M. G. Haehnelt, "Warm dark matter as a solution to the small scale crisis: New constraints from high redshift Lyman-α forest data," *Phys. Rev.* **D88** (2013) 043502, `arXiv:1306.2314 [astro-ph.CO]`.

[12] B. Audren, J. Lesgourgues, G. Mangano, P. D. Serpico, and T. Tram, "Strongest model-independent bound on the lifetime of dark matter," *JCAP* **1412** (2014) 028, `arXiv:1407.2418 [astro-ph]`

[13] H. Baer, K.-Y. Choi, J. E. Kim, and L. Roszkowski, "Dark matter production in the early Universe: beyond the thermal WIMP paradigm," *Phys. Rept.* **555** (2014) 1–60, `arXiv:1407.0017 [hep-ph]`.

[14] P. Gondolo and G. Gelmini, "Cosmic abundances of stable particles: Improved analysis," *Nucl. Phys.* **B360** (1991) 145–179.

[15] T. Nihei, L. Roszkowski, and R. Ruiz de Austri, "Towards an accurate calculation of the neutralino relic density," *JHEP* **05** (2001) 063, `arXiv:hep-ph/0102308 [hep-ph]`.

[16] S. P. Martin, "A Supersymmetry primer," `arXiv:hep-ph/9709356 [hep-ph]`. [Adv. Ser. Direct. High Energy Phys.18,1(1998)].

[17] R. Contino, "The Higgs as a Composite Nambu-Goldstone Boson," in *Physics of the large and the small, TASI 09, proceedings of the Theoretical Advanced Study Institute in Elementary Particle Physics, Boulder, Colorado, USA, 1-26 June 2009*, pp. 235–306. 2011. `arXiv:1005.4269 [hep-ph]`. `http://inspirehep.net/record/856065/files/arXiv:1005.4269.pdf`.

[18] H.-C. Cheng, "Introduction to Extra Dimensions," in *Physics of the large and the small, TASI 09, proceedings of the Theoretical Advanced Study Institute in Elementary Particle Physics, Boulder, Colorado, USA, 1-26 June 2009*, pp. 125–162. 2011. `arXiv:1003.1162 [hep-ph]`. `http://inspirehep.net/record/847930/files/arXiv:1003.1162.pdf`.

[19] G. C. Branco, P. M. Ferreira, L. Lavoura, M. N. Rebelo, M. Sher, and J. P. Silva, "Theory and phenomenology of two-Higgs-doublet models," *Phys. Rept.* **516** (2012) 1–102, `arXiv:1106.0034 [hep-ph]`.

[20] Y. Okada and L. Panizzi, "LHC signatures of vector-like quarks," *Adv. High Energy Phys.* **2013** (2013) 364936, `arXiv:1207.5607 [hep-ph]`.

[21] G. Jungman, M. Kamionkowski, and K. Griest, "Supersymmetric dark matter," *Phys.Rept.* **267** (1996) 195–373, `arXiv:hep-ph/9506380 [hep-ph]`.

[22] J. Pardo Vega and G. Villadoro, "SusyHD: Higgs mass Determination in Supersymmetry," *JHEP* **07** (2015) 159, `arXiv:1504.05200 [hep-ph]`.

[23] **CMS** Collaboration, "Search for supersymmetry in final states with missing transverse energy and 0, 1, 2, 3, or at least 4 b-quark jets in 8 TeV pp collisions using the variable AlphaT," Tech. Rep. CMS-PAS-SUS-12-028, CERN, Geneva, 2012. `https://cds.cern.ch/record/1494483`

[24] **LUX** Collaboration, D. S. Akerib *et al.*, "First results from the LUX dark matter experiment at the Sanford Underground Research Facility," *Phys. Rev. Lett.* **112** (2014) 091303, `arXiv:1310.8214 [astro-ph.CO]`.

[25] B. Acharya, M. Actis, T. Aghajani, G. Agnetta, J. Aguilar, *et al.*, "Introducing the CTA concept," *Astropart.Phys.* **43** (2013) 3–18.

[26] A. H. G. Peter, V. Gluscevic, A. M. Green, B. J. Kavanagh, and S. K. Lee, "WIMP physics with ensembles of direct-detection experiments," *Phys. Dark Univ.* **5-6** (2014) 45–74, `arXiv:1310.7039 [astro-ph.CO]`.

[27] **XENON** Collaboration, E. Aprile *et al.*, "First Dark Matter Search Results from the XENON1T Experiment," *Phys. Rev. Lett.* **119** no. 18, (2017) 181301, `arXiv:1705.06655 [astro-ph.CO]`.

[28] **Fermi-LAT** Collaboration, W. B. Atwood *et al.*, "The Large Area Telescope on the Fermi Gamma-ray Space Telescope Mission," *Astrophys. J.* **697** (2009) 1071–1102, `arXiv:0902.1089 [astro-ph.IM]`.

[29] Y. Bai, P. J. Fox, and R. Harnik, "The Tevatron at the Frontier of Dark Matter Direct Detection," *JHEP* **12** (2010) 048, `arXiv:1005.3797 [hep-ph]`.

[30] D. Abercrombie *et al.*, "Dark Matter Benchmark Models for Early LHC Run-2 Searches: Report of the ATLAS/CMS Dark Matter Forum," `arXiv:1507.00966 [hep-ex]`.

[31] **Muon g-2** Collaboration, G. W. Bennett *et al.*, "Final Report of the Muon E821 Anomalous Magnetic Moment Measurement at BNL," *Phys. Rev.* **D73** (2006) 072003, `arXiv:hep-ex/0602035 [hep-ex]`.

[32] **Muon g-2** Collaboration, A. Chapelain, "The Muon g-2 experiment at Fermilab," *EPJ Web Conf.* **137** (2017) 08001, `arXiv:1701.02807 [physics.ins-det]`.

[33] **J-PARC g-2** Collaboration, T. Mibe, "New g-2 experiment at J-PARC," *Chin. Phys.* **C34** (2010) 745–748.

Enrico Maria Sessolo